

These results corroborate previous observations (Boeyens & Dobson, 1987; Dobson, 1986): 9-ane-N₃, 9-ane-S₃ and 9-ane-N₂S when complexed with Ni^{II} adopt a similar conformation along the BC-TBC pseudorotational cycle. When 9-ane-N₂S is complexed with Cu^{II}, a different intermediate conformation is energetically preferred.

Concluding remarks

This communication completes the survey of ring conformations and the mapping of symmetrical forms on geometrical surfaces for graphical analysis of unknown configurations, from crystallographic coordinates. The procedure has been automated in the meantime and our FORTRAN program, *CONFOR*, which identifies the nearest symmetrical form and quantitatively defines the conformation as a linear combination of primitive forms, is available from the authors.

References

BOESSENKOOL, I. K. & BOEYENS, J. C. A. (1980). *J. Cryst. Mol. Struct.* **10**, 11–18.

- BOEYENS, J. C. A. (1978). *J. Cryst. Mol. Struct.* **8**, 317–320.
 BOEYENS, J. C. A. & DOBSON, S. M. (1987). In *Stereochemistry of Organometallic and Inorganic Compounds*, Vol. 2, edited by I. BERNAL. Amsterdam: Elsevier.
 BOEYENS, J. C. A., DOBSON, S. M. & HANCOCK, R. D. (1985). *Inorg. Chem.* **24**, 3073–3076.
 BOEYENS, J. C. A. & EVANS, D. G. (1989). *Acta Cryst.* **B45**, 577–581.
 CREMER, D. & POPLE, J. A. (1975). *J. Am. Chem. Soc.* **97**, 1354–1358.
 DALE, J. (1973a). *Acta Chem. Scand.* **27**, 1115–1129.
 DALE, J. (1973b). *Acta Chem. Scand.* **27**, 1130–1148.
 DOBSON, S. M. (1986). *A Crystallographic and Thermodynamic Study of Macrocyclic Complexes*, PhD Thesis, Univ. of the Witwatersrand, South Africa.
 EVANS, D. G. & BOEYENS, J. C. A. (1988). *Acta Cryst.* **B44**, 663–671.
 EVANS, D. G. & BOEYENS, J. C. A. (1989). *Acta Cryst.* **B45**, 581–590.
 GLASS, R. S., WILSON, G. S. & SETZER, W. N. (1980). *J. Am. Chem. Soc.* **102**, 5068–5069.
 HART, S. M., BOEYENS, J. C. A., MICHAEL, J. P. & HANCOCK, R. D. (1983). *J. Chem. Soc. Dalton Trans.* pp. 1601–1606.
 HENDRICKSON, J. B. (1964). *J. Am. Chem. Soc.* **86**, 4854–4866.
 HENDRICKSON, J. B. (1967). *J. Am. Chem. Soc.* **89**, 7047–7061.
 PETTIT, G. H., DILLEN, J. & GEISE, H. J. (1983). *Acta Cryst.* **B39**, 648–651.
 SETZER, W. N., OGLE, C. A., WILSON, G. S. & GLASS, R. S. (1983). *Inorg. Chem.* **22**, 266–271.
 ZOMPA, L. J. & MARGULIS, T. N. (1978). *Inorg. Chim. Acta*, **28**, L157–159.

Acta Cryst. (1990). **B46**, 532–538

Electrostatic Properties of Cytosine Monohydrate from Diffraction Data

BY H.-P. WEBER* AND B. M. CRAVEN†

Crystallography Department, University of Pittsburgh, Pittsburgh, PA 15260, USA

(Received 26 September 1988; accepted 22 January 1990)

Abstract

The charge density distribution in deuterated cytosine monohydrate [4-(²H₂)-amino-2(1H)-(1-²H)-pyrimidinone], C₄H₂D₃N₃O.D₂O, *M_r* = 134.15, monoclinic, *P*2₁/*c*, *a* = 7.714 (1), *b* = 9.825 (1), *c* = 7.506 (2) Å, β = 100.52 (1)°, *Z* = 4, has been determined from 1432 X-ray reflections [sinθ/λ < 1.15 Å⁻¹, Mo *K*α, λ = 0.7093 (1) Å] collected at 82 (2) K. Least-squares structure refinement assuming Stewart's rigid pseudoatom model gave *R*(*F*) = 0.041, with all nuclear positions and H/D anisotropic thermal parameters having fixed values previously determined by neutron diffraction. The cytosine and water molecules are both electrically neutral within

experimental error (0.09 e). Molecular dipole moments are μ = 8.0 (1.4) debye for cytosine and 2.3 (3) debye for water. For the doubly hydrogen-bonded cytosine dimer (N1—D1⋯N3', N4—D4⋯O2') isolated from the crystal, the electrostatic energy of interaction is estimated to be -96 (27) kJ mol⁻¹. Maps of the electrostatic potential for molecules isolated from the crystal indicate that the electronegativity of the hydrogen-bonding acceptor sites can be ranked with the water O atom, cytosine N(3) and carbonyl O(2) in decreasing order.

Introduction

The crystal structures of cytosine and its monohydrate have received considerable attention because of the importance of cytosine as a component of the

* Present address: Institute de Cristallographie, Université de Lausanne, BSP Dorigny, CH-1015, Lausanne, Switzerland.

† To whom correspondence should be addressed.

nucleic acids. The X-ray crystal structure of cytosine monohydrate was first determined by Jeffrey & Kinoshita (1963). The structure was later redetermined from diffractometer data by McClure & Craven (1973) in order to resolve questions concerning the possible effects of hydrogen bonding on the bond lengths in the anhydrous (Barker & Marsh, 1964) and hydrated crystals. Further details of the molecular geometry were obtained from neutron diffraction data collected for the monohydrate at 82 K (Weber, Craven & McMullan, 1980; hereafter WCM). In order to improve the quality of the neutron data, the hydrogen-bonded protons were substituted by deuterium. The results of WCM form the basis for the presently reported study of the charge density distribution in the crystal and the derived electrostatic properties of the component molecules. This study was carried out with high-resolution X-ray diffraction data collected at 82 (2) K, using a crystal from the same batch of deuterated material prepared by WCM. A parallel study of a completely protonated crystal with X-ray data collected at 97 K has been carried out by Eisenstein (1988).

Experimental

Crystals of deuterated cytosine monohydrate were grown as described by WCM. The crystal selected for X-ray data collection was a plate developed on {100}, elongated on *b* and exhibiting {010} and $\{\bar{1}02\}$. The dimensions were $0.15 \times 0.27 \times 0.50$ mm. The crystal was mounted on a glass pin enclosed in a thin-glass dome on a copper base which was in contact with a reservoir of liquid nitrogen and this assembly was in a cryostat with beryllium walls. The crystal was oriented with *b* approximately along the φ axis of a computer-controlled Picker FACS-I diffractometer. All X-ray data were collected using graphite-monochromated Mo $K\alpha$ radiation ($\lambda = 0.7093$ Å). The crystal temperature was estimated to be 82 (2) K by comparison of the unit-cell parameters with values measured at four temperatures in the range 72–92 K by WCM using neutron diffraction.* The X-ray unit-cell parameters were obtained by a least-squares fit of $\sin^2\theta$ values for 31 reflections with $0.57 < \sin\theta/\lambda < 0.88$ Å⁻¹. The results were $a = 7.714$ (1), $b = 9.825$ (1), $c = 7.506$ (2) Å, $\beta = 100.52$ (1)°. Integrated intensities were measured by an $\omega/2\theta$ step-scan procedure for 9107 reflections

with $\sin\theta/\lambda < 1.15$ Å⁻¹, including the measurement of all non-symmetry-related reflections at least twice, most in different quadrants of reciprocal space. The scan width was $\Delta 2\theta = (2.5 + 0.9\tan\theta)^\circ$ and the step-scan interval in 2θ was 0.04° . Two monitor reflections, which were measured after every 45 reflections, showed no significant variation. Azimuthal scans measured for reflections 020 (strong) and 081 (weak) indicated that the data were not seriously affected by X-ray extinction. Scan profiles were inspected using a computer-graphics procedure (Weber & McMullan, 1979) in order to estimate peak widths and backgrounds. Integrated intensities were corrected for X-ray absorption (de Meulenaer & Tompa, 1965; Templeton & Templeton, 1973) assuming the absorption coefficient $\mu = 0.14$ mm⁻¹, although the resulting transmission factors were all within a narrow range (0.93–0.97). For symmetry-related and multiply-measured reflections, the value for $R_{\text{merge}} = (\sum|F^2 - \langle F^2 \rangle|)/(\sum\langle F^2 \rangle)$ was 0.028. Variances in F^2 were estimated from deviations from the mean using 44 reflections for which there were at least 10 observations. These variances in individual reflections were then fitted by least squares to the expression $\sigma(F^2) = a + bF^4$. For F^2 on the scale determined after the structure analysis, this gave $a = 95$ (2) and $b = 3.695$ (2) $\times 10^{-4}$. With these variances, the total number of non-symmetry-related reflections (4304) included 1432 with $F^2 > 2.5\sigma$. Only the latter were included in the crystal structure refinement.

Structure refinement

The charge density distribution in the crystal structure was determined by full-matrix least-squares refinement assuming the rigid pseudoatom model of Stewart (1976). The refinement and subsequent calculations of derived electrostatic properties were carried out with the computer programs of Craven, Weber & He (1987). The calculations of electrostatic potential were based on a procedure developed by Stewart (1983) and summarized by He (1984).

Each pseudoatom was assumed to have an invariant core consisting of an isolated neutral Hartree-Fock atom or a spherically averaged bonded H/D atom (Stewart, Davidson & Simpson, 1965). Corresponding X-ray scattering factors were taken from Cromer, Waber & Ibers (1974). The variable component for describing the net charge and asphericity of the pseudoatom was assumed to be given by a linear combination of terms, each consisting of the product of a Slater-type density function and a multipole angular function weighted by a variable electron population parameter. The multipole expansion was complete up to octapoles (quadrupoles for H/D). Explicit functions and scattering factors for C, N, O and H/D, including the

* During crystal cooling from room temperature, we did not observe a phase transformation near 140 K as described by Eisenstein (1988). We have also used a Mettler TA3000 system to carry out differential calorimetric scans with a powder sample of fully protonated cytosine hydrate. Over the range from 103 K to room temperature, there was no indication of a phase transformation. A small endothermic peak at 273 K was attributed to the thawing of water adsorbed on the sample surface.

normalization factors of Hansen & Coppens (1978), were those given by Epstein, Ruble & Craven (1982). Radial exponents in the single Slater-type function assumed for all pseudoatoms of the same kind were assigned fixed values $\alpha = 6.20, 7.28, 8.25, 4.35 \text{ \AA}^{-1}$ for C, N, O and H/D respectively. These are close to the standard values of Hehre, Stewart & Pople (1969).

The structure model for refinement involved 207 variables, consisting of 54 anisotropic thermal parameters for C, N and O, and 153 electron population parameters. All nuclear positional parameters together with anisotropic thermal parameters for H/D were assigned fixed values determined from neutron diffraction by WCM. The function minimized by least squares was $\sum w\Delta^2$ where $w =$

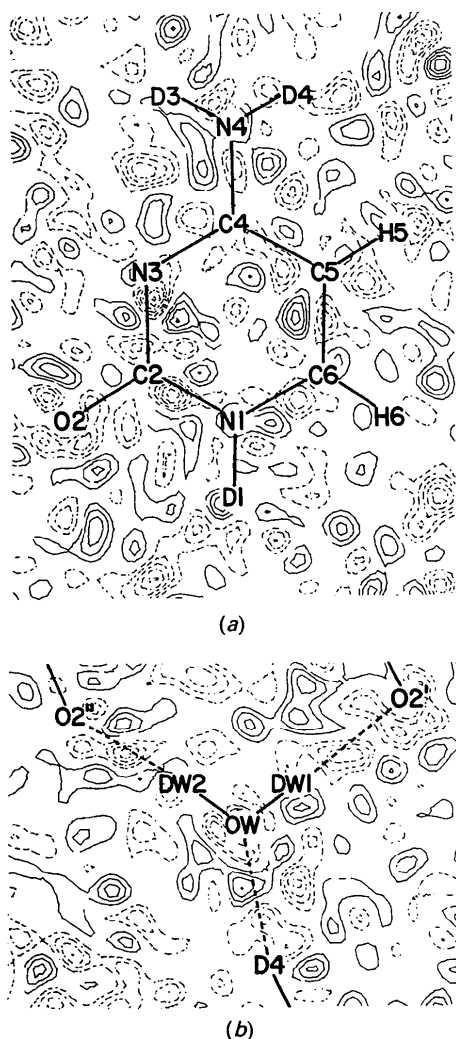


Fig. 1. Difference Fourier synthesis of residual electron density in the planes through (a) the cytosine molecule, (b) the water molecule. The contour interval is 0.05 e \AA^{-3} with the zero contour omitted. The average value for $\sigma(\rho) = 0.07 \text{ e \AA}^{-3}$.

Table 1. Anisotropic thermal parameters ($\text{\AA}^2 \times 10^4$)

These are for temperature factors of the form $T = \exp(-2\pi^2 \sum_i \sum_j U_{ij} a_i^* a_j^*)$. For each atom, values from X-ray diffraction are given above those from neutron diffraction (Weber, Craven & McMullan, 1980). For H/D nuclei, only the neutron values are given.

	U_{11}	U_{22}	U_{33}	U_{12}	U_{13}	U_{23}
N(1)	73 (7)	68 (10)	136 (8)	3 (6)	42 (6)	-7 (7)
	80 (3)	51 (3)	115 (3)	4 (2)	38 (2)	1 (2)
C(2)	83 (5)	77 (8)	108 (6)	-8 (6)	36 (5)	4 (7)
	70 (3)	50 (4)	83 (4)	4 (3)	34 (3)	5 (3)
O(2)	87 (6)	123 (9)	154 (7)	7 (8)	57 (5)	6 (9)
	84 (4)	83 (4)	150 (5)	-2 (4)	56 (3)	-1 (3)
N(3)	97 (6)	74 (9)	121 (7)	11 (6)	36 (6)	-1 (6)
	74 (3)	43 (3)	117 (3)	4 (2)	39 (2)	4 (2)
C(4)	74 (6)	79 (9)	115 (7)	-2 (6)	39 (5)	0 (6)
	70 (4)	52 (4)	108 (4)	4 (3)	35 (3)	1 (3)
N(4)	110 (6)	75 (9)	161 (8)	-7 (6)	56 (6)	4 (7)
	96 (3)	59 (3)	157 (4)	-4 (2)	58 (2)	5 (2)
C(5)	96 (6)	80 (8)	150 (7)	7 (7)	60 (5)	7 (8)
	90 (4)	56 (4)	123 (4)	10 (3)	49 (3)	2 (3)
C(6)	110 (7)	63 (9)	141 (8)	10 (6)	54 (6)	-12 (7)
	90 (4)	46 (3)	112 (2)	3 (3)	62 (3)	-6 (3)
O(W)	104 (6)	147 (9)	145 (8)	20 (6)	47 (6)	11 (8)
	89 (4)	110 (5)	158 (5)	2 (3)	51 (4)	12 (4)
D(1)	165 (6)	99 (5)	225 (7)	-18 (4)	75 (4)	5 (4)
D(3)	191 (6)	95 (6)	293 (8)	18 (4)	95 (5)	-7 (4)
D(4)	138 (5)	165 (6)	252 (7)	-17 (4)	85 (4)	1 (4)
H(5)	205 (11)	210 (12)	409 (16)	-5 (9)	-180 (10)	-7 (10)
H(6)	236 (12)	117 (10)	280 (13)	47 (8)	89 (9)	-7 (8)
DW(1)	188 (6)	200 (7)	203 (6)	23 (5)	38 (4)	26 (5)
DW(2)	206 (6)	194 (7)	248 (7)	-22 (5)	118 (5)	35 (5)

$1/\sigma^2(F)$ and $\Delta = |F_o| - |F_c|$. In the final cycles of refinement, the scale factor was constrained so that the contents of the unit cell would be electrically neutral. The change in scale factor from the unconstrained value was -2.1% . No X-ray extinction parameters were included. Refinement converged with no parameter shift exceeding 0.05σ , $R(F) = 0.041$, $wR(F) = 0.030$ and $S = 1.05$.* The final difference Fourier synthesis of residual electron density (Fig. 1), shows features ranging from 0.26 to $-0.31 (8) \text{ e \AA}^{-3}$ which are no more than marginally significant. Final values for the anisotropic thermal parameters and electron population parameters are in Tables 1 and 2. Final structure factors† are listed with values of F^2 so as to include the 2601 weak reflections and those with negative measured intensity which were not used in refinement.

Comparison of C, N and O anisotropic thermal parameters obtained from X-ray and neutron diffraction (WCM) shows good agreement except for U_{22} . However, as can be seen in Table 1, values ($U_x - U_N$) are mostly positive with the root-mean-square values $0.0010 (9)$, $0.0026 (8)$ and $0.0012 (13) \text{ \AA}^2$ for U_{11} , U_{22} and U_{33} respectively (σ 's from the statistical distribution). It was because of these systematic differences that the final structure

* $R(F) = \sum |\Delta| / \sum |F_o|$, $wR(F) = (\sum w\Delta^2 / \sum F^2)^{1/2}$, $S = [\sum w\Delta^2 / (m-n)]^{1/2}$.

† A list of structure factors has been deposited with the British Library Document Supply Centre as Supplementary Publication No. SUP 52706 (45 pp.). Copies may be obtained through The Technical Editor, International Union of Crystallography, 5 Abbey Square, Chester CH1 2HU, England.

Table 2. *Electron population parameters* ($\times 100$ for p_v ; $\times 10$ for d_j, q_j, o_j)

These correspond to the normalized functions referred to crystal axes a, b, c^* , as described in the *Appendix* by Epstein, Ruble & Craven (1982).

	p_v	d_1	d_2	d_3	q_1	q_2	q_3	q_4	q_5	o_1	o_2	o_3	o_4	o_5	o_6	o_7
N(1)	31 (6)	-2 (2)	-3 (3)	-4 (2)	21 (6)	-3 (6)	-1 (5)	14 (5)	-28 (4)	21 (4)	-1 (5)	-9 (5)	-7 (4)	3 (4)	8 (4)	3 (4)
O(2)	14 (3)	-13 (2)	1 (2)	2 (2)	2 (4)	-5 (5)	3 (4)	-9 (5)	-1 (4)	5 (3)	8 (4)	1 (4)	-2 (4)	-2 (4)	-7 (4)	7 (4)
N(3)	23 (4)	-6 (2)	9 (2)	10 (2)	-9 (4)	-12 (4)	4 (4)	3 (4)	-2 (4)	20 (4)	-8 (4)	0 (4)	-8 (4)	9 (4)	-2 (4)	1 (4)
C(4)	3 (5)	-6 (3)	2 (3)	9 (3)	5 (4)	2 (4)	-15 (4)	-2 (4)	-34 (4)	-40 (5)	4 (5)	21 (5)	4 (5)	-3 (5)	3 (4)	5 (4)
N(4)	-7 (8)	-5 (3)	-3 (3)	5 (3)	-1 (5)	1 (5)	4 (4)	3 (5)	6 (4)	24 (4)	-7 (4)	-13 (4)	-4 (5)	-6 (4)	-3 (4)	0 (4)
C(5)	-6 (7)	3 (3)	15 (4)	1 (3)	-1 (4)	-3 (5)	-9 (4)	-9 (4)	-19 (4)	32 (4)	1 (5)	-16 (4)	9 (6)	1 (5)	-17 (5)	-10 (4)
C(6)	15 (8)	17 (3)	2 (4)	-20 (3)	-13 (6)	-1 (4)	-28 (4)	10 (4)	-22 (4)	-28 (5)	1 (5)	20 (5)	-8 (5)	-2 (5)	-1 (5)	12 (4)
O(W)	17 (6)	-14 (3)	-2 (3)	-10 (3)	1 (5)	-17 (4)	3 (4)	7 (5)	2 (5)	-7 (4)	-7 (4)	-8 (4)	-3 (4)	8 (4)	2 (4)	5 (4)
D(1)	-29 (4)	28 (3)	34 (4)	1 (3)	-13 (4)	23 (4)	18 (4)	6 (4)	5 (4)							
D(3)	-22 (4)	18 (3)	-15 (5)	-11 (3)	-13 (4)	-7 (4)	4 (4)	16 (4)	-33 (4)							
D(4)	-8 (4)	-35 (5)	-8 (4)	11 (4)	21 (4)	12 (5)	-15 (4)	0 (4)	-12 (4)							
H(5)	-9 (4)	-17 (5)	-3 (4)	3 (4)	4 (4)	7 (4)	22 (4)	-27 (4)	-25 (5)							
H(6)	-27 (4)	-8 (4)	11 (5)	0 (4)	-7 (4)	-7 (4)	-22 (4)	30 (4)	8 (4)							
DW(1)	-5 (4)	-13 (4)	11 (4)	-28 (4)	-16 (4)	-6 (14)	18 (5)	0 (4)	2 (4)							
DW(2)	-4 (5)	-15 (4)	8 (3)	28 (4)	10 (4)	4 (4)	-9 (5)	14 (4)	19 (4)							

refinement with X-ray data included the C, N and O anisotropic thermal parameters as variables.

The maps of the molecular deformation charge density and electrostatic potential for a static arrangement of pseudoatoms (Figs. 2 and 3) were constructed from the functions given by Epstein *et al.* (1982) and population parameters from Table 2.

Discussion

The net electronic charge for each pseudoatom is the negative value of the monopole population parameter, p_v . Thus a positive p_v (Table 2) represents an excess of electron density. However, values of population parameters for individual pseudoatoms are of limited physical significance because they are model-dependent. The sum $-\sum p_v$ over the pseudoatoms of a molecule gives an estimate of the total molecular charge. Molecular properties such as this are of more interest. They are not as strongly influenced by the mode of partitioning the total charge density as are the individual pseudoatom properties. In the crystal structure of cytosine monohydrate, net charges on the component molecules are small [-0.08 (9) e for D_2O ; equal and opposite for cytosine] and not significant in terms of the experimental error.

The deformation charge density, which in our experience is a property very sensitive to systematic errors in the data or deficiencies in the structure model, has a similar distribution in our maps (Fig. 2) and those of Eisenstein (1988). In making this comparison, it is emphasized that Eisenstein (1988) collected her X-ray data at a higher temperature (97 K) and thus could not make direct use of the neutron diffraction results of WCM. Also, she assumed the structure model proposed by Hirshfeld (1977). This model becomes equivalent to that of Stewart (1976) which we used, provided that the series of deformation terms is sufficiently extended. In the present case, the Hirshfeld model was used with maximum $n = 4$, corresponding to an incomplete multipole

expansion at the hexadecapole level, whereas our multipole expansion was complete but extended only to the octapole level (quadrupole for H/D). Also, Eisenstein constrained the deformation density terms for atoms N3, C4 and C5 to have local symmetry mm and H atoms to have axial symmetry, whereas we have imposed no such constraints. The differences in the models assumed in the two studies can be seen most notably as differences in the peak shapes in the resulting deformation density maps.

The deformation density near the carbonyl O2 atom is of interest because this O atom forms a long C—O bond [1.262 (1) Å] and in the crystal it takes part in three H(D) bonds. As can be seen from Figs. 2(a) and 2(b), the deformation density is asymmetrical around O2 in the plane through O2 normal to the C—O bond. Here there are two peaks, the larger occurring along one of the two H(D) bonds formed with water, while the smaller lies between the other H(D) bonds. Possibly, the orientation of these peaks is caused by the intermolecular H(D) bonding, since it does not conform to the symmetry of the isolated molecule. However, the effect could also be caused by an incomplete deconvolution of the charge density from the thermal vibrations of the O atoms. This deconvolution can be unreliable for carbonyl O atoms (He, Swaminathan, Craven & McMullan, 1988).

The water molecule forms three H(D) bonds in a flattened pyramidal configuration, two of these as donor with different carbonyl O atoms, and one as acceptor with the cytosine amino group. The deformation density at the water OW on the acceptor side consists of a single broad peak ($1.2 \text{ e } \text{Å}^{-3}$, Fig. 2c). As shown in Fig. 2(d), this peak extends asymmetrically above and below the plane of the molecule, tending to be aligned with the H(D)-bonding OW...D4 direction. Similar features were observed in the deformation density in the crystal structure of oxalic acid dihydrate (Stevens & Coppens, 1980), where the water molecule also forms three hydrogen bonds in a pyramidal arrangement, and in *trans*-2,5-

dimethyl-3-hexene-2,5-diol hemihydrate (Van der Wal, van Duijnen & Vos, 1983). However, in the latter case, polarization of O-atom lone-pair density, which seemed to occur in the experimental maps, was absent in the corresponding theoretical maps.

The molecular dipole moments calculated from the distribution of pseudoatom monopole and dipole population parameters (Table 2) are $|\mu| = 8.0$ (1.4) debye for cytosine and 2.3 (3) debye for the water molecule. For cytosine, μ makes an angle 9 (10)° with the O2=C2 bond. For water, μ makes an angle 19 (8)° with the D—O—D bisector and 13 (7)° with the molecular plane, these deviations from the symmetry of an isolated molecule being

insignificant. The values for $|\mu|$ obtained by Eisenstein (1988) are smaller (5.8 debye for cytosine and 1.58 debye for water), perhaps because of assumptions which were needed to determine the charge distribution around the H atoms. We are unaware of other experimental estimates of $|\mu|$ for cytosine. However, Palmer, Wheeler, Kwiatkowski & Lesyng (1983) report a value 7.56 debye obtained from an *ab initio* molecular-orbital calculation. The orientations of this theoretical and our experimental μ agree within 10° . For water, our crystallographic value for $|\mu|$ agrees within the estimated error with the microwave value 1.84 debye (Dyke & Muentzer, 1973).

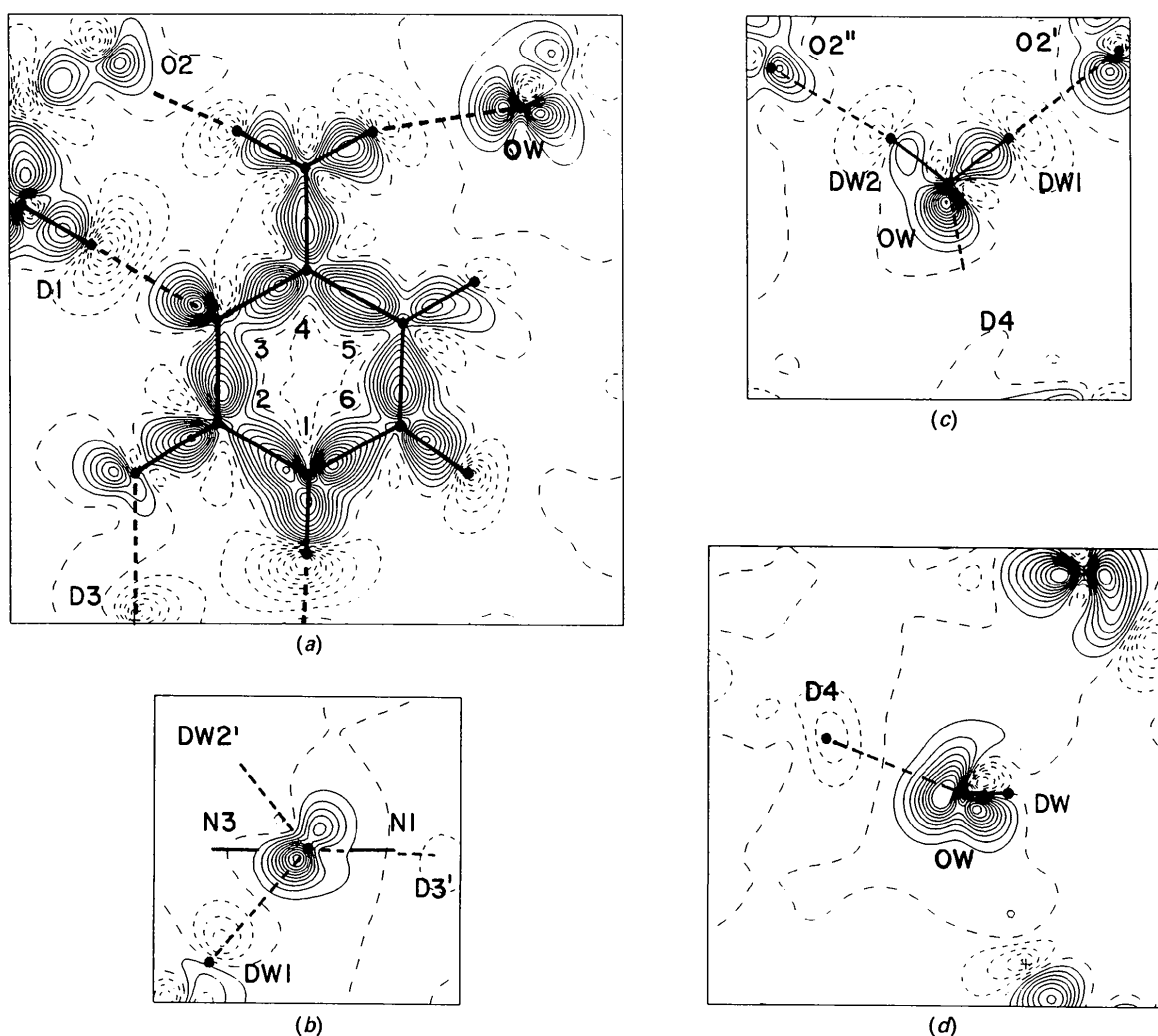


Fig. 2. Deformation charge density for static arrays of pseudoatoms as in the crystal structure. Contours at intervals $0.1 \text{ e } \text{\AA}^{-3}$, with the zero contour dashed and negative contours dotted. (a) Plane of the cytosine molecule. (b) Section normal to the C2—O2 bond, with O2 (center) 0.2 \AA below the plane of the section. The trace of the plane of the cytosine ring is horizontal. Heavy dashed lines indicate H(D) bonds to DW2' and D3' (above this section) and DW1 (close to this section). (c) Plane of the water molecule. Heavy dashed lines indicate H(D) bonds to O2 atoms (both 0.2 \AA below this section) and D4 (0.7 \AA above). (d) Section through the water OW and bisecting the O—D bond directions.

The energies of interaction of pairs of molecules taken from the crystal structure of deuterated cytosine monohydrate have already been reported and discussed by Spackman, Weber & Craven (1988). These energies were derived in part from electron-gas theory and in part from our presently described experimental charge density distribution. Thus for the hydrogen-bonded cytosine dimer ($N1-D1\cdots N3'$, $N4-D4\cdots O2'$) as found in the crys-

tal structure (see Spackman *et al.*, 1988; Fig. 4), the experimental electrostatic energy of interaction was found to be -96 (27) kJ mol^{-1} and the total energy -75 kJ mol^{-1} .

The maps of electrostatic potential (Fig. 3) are for molecules of cytosine and water isolated from the crystal structure. Electronegative regions where a positively charged probe would have low energy are to be found near the hydrogen-bonding acceptor

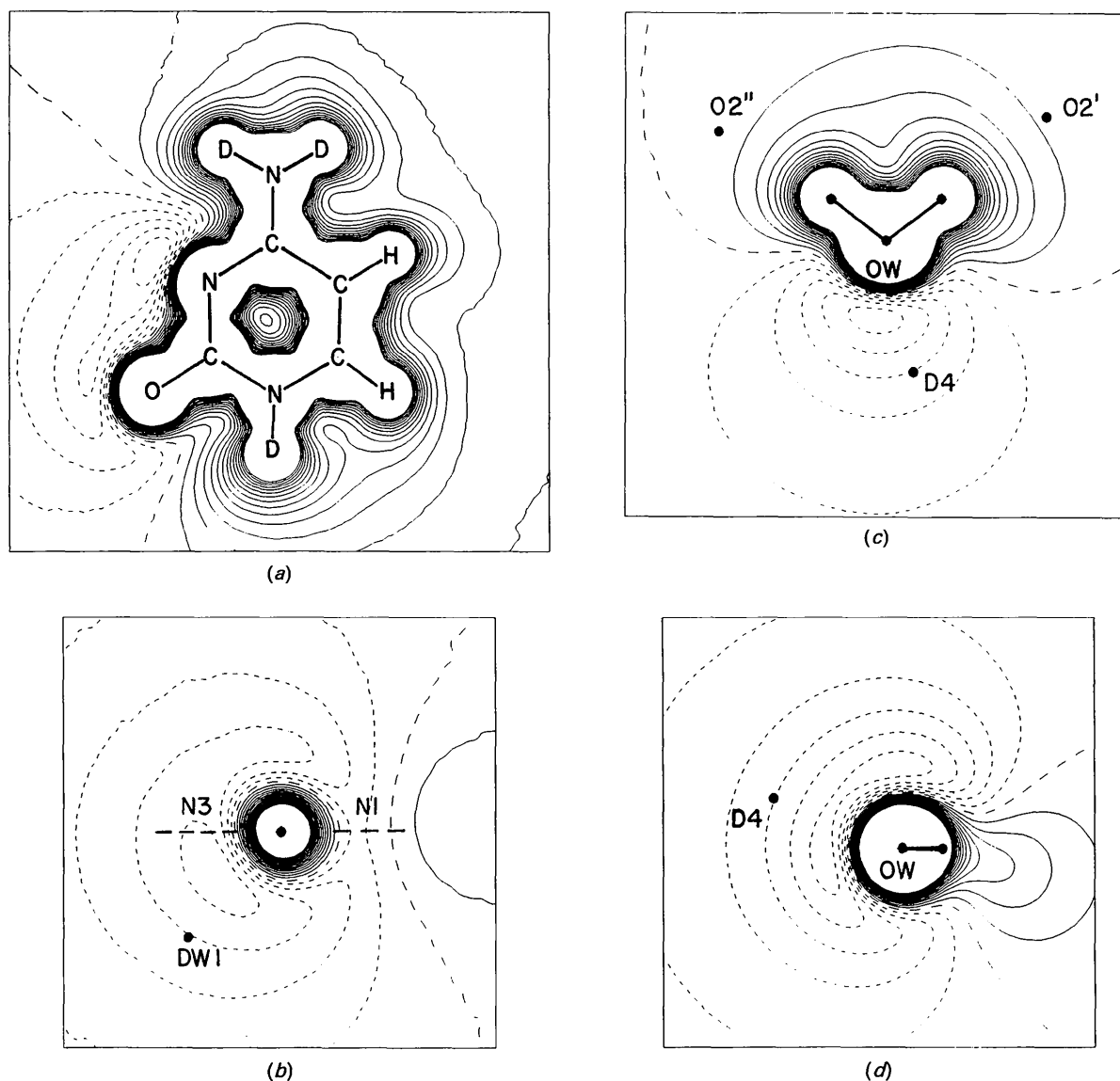


Fig. 3. Electrostatic potential for static arrays of pseudoatoms, including the contributions from the Hartree-Fock core of each pseudoatom. The contour interval is $0.05 \text{ e } \text{\AA}^{-1}$ with the zero contour dashed and negative contours dotted. Negative regions are of low energy for a positive point charge. $0.1 \text{ e } \text{\AA}^{-1} = 138.9 \text{ kJ mol}^{-1} = 33.2 \text{ kcal mol}^{-1}$. (a) A cytosine molecule isolated from the crystal structure. (b) A cytosine molecule isolated from the crystal structure and shown in the same section as Fig. 2(b), with O2 at the center. The position which would be occupied by DW1 is indicated. (c) A water molecule isolated from the crystal structure and shown in the same section as Fig. 2(c). The positions which would be occupied by H(D)-bonded atoms are indicated. (d) A water molecule isolated from the crystal structure and shown in the same section as Fig. 2(d). The position which would be occupied by the H(D)-bonded D4 is indicated.

groups in both molecules. The most extensive electropositive regions are near the hydrogen-bonded donor D atoms. In this respect, the maps are similar to those obtained by Stewart (1982) from the diffraction data for imidazole (Epstein *et al.*, 1982; McMullan, Epstein, Ruble & Craven, 1979) and 9-methyladenine (Craven & Benci, 1981; McMullan, Benci & Craven, 1980). Unlike the maps for these molecules, the results for cytosine monohydrate allow a direct comparison of the negative electrostatic potential at three hydrogen-bonding acceptor sites with different chemical characteristics. From a comparison of the two O atoms (Fig. 3), it can be seen that the minimum is deeper at the water O atom (-379 kJ mol^{-1}) than at the carbonyl O atom (-292 kJ mol^{-1}). Also, for the cytosine molecule with adjacent acceptor sites at N(3) and the carbonyl O atom, N(3) is the more electronegative (-414 kJ mol^{-1}). This indicates that N(3) would be the preferred site for the hydrogen bonding of cytosine. In contrast, earlier maps based on *ab initio* molecular-orbital calculations for cytosine by Bonaccorsi, Pullman, Scrocco & Tomasi (1972) showed both sites to be almost equally electronegative (-391 versus -363 kJ mol^{-1}). Such a difference might arise because the theoretical map is derived for an isolated molecule which is not hydrogen bonded, whereas the experimental map is for a molecule isolated from the crystal structure in a state already prepared for hydrogen bonding at all donor and acceptor sites.

The electrostatic potential around the water molecule is diffuse (Fig. 3c). As noted in the case of the deformation charge density, the electronegative region (Fig. 3d) is asymmetric with respect to the molecular plane. Thus the electrostatic potential for the water molecule removed from the crystal seems to retain the effect of the H(D) bonding with the electropositive D4 which occurs in the crystal environment.

This work was supported by grants GM-22548, HL-20350 and GM-39513 from the National Institutes of Health. Facilities for X-ray diffraction data collection and initial data processing were made available to HPW as a visitor to the Chemistry Department, Brookhaven National Laboratory, where help and encouragement was kindly provided

by Dr Richard McMullan. We are grateful to Dr S. Swaminathan for some of the later calculations and also to Mrs Joan Klinger for technical assistance. We thank Dr Miriam Eisenstein for sending us her results in advance of publication.

References

- BARKER, D. L. & MARSH, R. E. (1964). *Acta Cryst.* **17**, 1581–1587.
 BONACCORSI, R., PULLMAN, A., SCROCCO, E. & TOMASI, J. (1972). *Theor. Chim. Acta*, **24**, 51–60.
 CRAVEN, B. M. & BENCI, P. (1981). *Acta Cryst.* **B37**, 1584–1591.
 CRAVEN, B. M., WEBER, H.-P. & HE, X. M. (1987). *The POP Refinement Procedure*. Tech. Rep. Department of Crystallography, Univ. of Pittsburgh, USA.
 CROMER, D. T., WABER, J. T. & IBERS, J. A. (1974). *International Tables for X-ray Crystallography*, Vol. IV, pp. 71–147. Birmingham: Kynoch Press. (Present distributor Kluwer Academic Publishers, Dordrecht.)
 DYKE, T. R. & MUENTER, J. S. (1973). *J. Chem. Phys.* **59**, 3125–3127.
 EISENSTEIN, M. (1988). *Acta Cryst.* **B44**, 412–426.
 EPSTEIN, J., RUBLE, J. R. & CRAVEN, B. M. (1982). *Acta Cryst.* **B38**, 140–149.
 HANSEN, N. K. & COPPENS, P. (1978). *Acta Cryst.* **A34**, 909–921.
 HE, X. M. (1984). PhD Dissertation, Univ. of Pittsburgh, USA.
 HE, X. M., SWAMINATHAN, S., CRAVEN, B. M. & MCMULLAN, R. K. (1988). *Acta Cryst.* **B44**, 271–281.
 HEHRE, W. J., STEWART, R. F. & POPLE, J. A. (1969). *J. Chem. Phys.* **51**, 2657–2664.
 HIRSHFELD, F. (1977). *Isr. J. Chem.* **16**, 226–229.
 JEFFREY, G. A. & KINOSHITA, Y. (1963). *Acta Cryst.* **16**, 20–28.
 MCCLURE, R. J. & CRAVEN, B. M. (1973). *Acta Cryst.* **B29**, 1234–1238.
 MCMULLAN, R. K., BENCI, P. & CRAVEN, B. M. (1980). *Acta Cryst.* **B36**, 1424–1430.
 MCMULLAN, R. K., EPSTEIN, J., RUBLE, J. R. & CRAVEN, B. M. (1979). *Acta Cryst.* **B25**, 688–691.
 MEULENAER, J. DE & TOMPA, H. (1965). *Acta Cryst.* **19**, 1014–1018.
 PALMER, M. H., WHEELER, J. R., KWIATKOWSKI, J. S. & LESYNG, B. (1983). *J. Mol. Struct.* **92**, 283–302.
 SPACKMAN, M. A., WEBER, H.-P. & CRAVEN, B. M. (1988). *J. Am. Chem. Soc.* **110**, 775–782.
 STEVENS, E. D. & COPPENS, P. (1980). *Acta Cryst.* **B36**, 1864–1876.
 STEWART, R. F. (1976). *Acta Cryst.* **A32**, 565–574.
 STEWART, R. F. (1982). *God. Jugosl. Cent. Kristallogr.* **17**, 1–24.
 STEWART, R. F. (1983). Unpublished work.
 STEWART, R. F., DAVIDSON, E. R. & SIMPSON, W. T. (1965). *J. Chem. Phys.* **42**, 3175–3187.
 TEMPLETON, L. K. & TEMPLETON, D. H. (1973). *Am. Crystallogr. Assoc. Meet.*, Storrs, Connecticut, Abstracts, p. 143.
 VAN DER WAL, R. J., VAN DULINEN, P. T. & VOS, A. (1983). *Acta Cryst.* **B39**, 646–647.
 WEBER, H.-P., CRAVEN, B. M. & MCMULLAN, R. K. (1980). *Acta Cryst.* **B36**, 645–649.
 WEBER, H.-P. & MCMULLAN, R. K. (1979). Unpublished work.